Volume 22, No 1 | International Journal of Radiation Research, January 2024

Impact of reconstruction algorithms on the success rate and quality of automatic airway segmentation in children under ultra-low-dose chest CT scanning

J. Sun[1], H. Li[1], Z. Liu[1], S. Wang[2], Y. Peng[1*]

[1]*Department of Radiology, Beijing Children's Hospital, Capital Medical University, National Center for Children's Health, Beijing 100045, China*

[2]*Department of Medical Imaging, Children's Hospital of Xinjiang Uygur Autonomous Region, Xinjiang Hospital of Beijing Children's Hospital, Urumqi 830000, China*

► ***Original article***

Corresponding author:
Yun Peng, Ph.D.,
E-mail:
ppengyun@hotmail.com

Received: December 2022
Final revised: April 2023
Accepted: June 2023

Int. J. Radiat. Res., January 2024; 22(1): 171-177

DOI: 10.52547/ijrr.21.24

Keywords: *CT, pediatrics, deep learning, image processing, computer-assisted.*

ABSTRACT

Background: To investigate the success rate and quality of automatic airway segmentation using ultra-low dose CT (ULD-CT) images of different reconstruction algorithms. ***Materials and Methods:*** Fifty two children who underwent chest ULD-CT were divided into three groups for analysis based on age: group A (n=13, age, 1-2years), group B (n=19, age, 3-6years) and group C (n=20, age, 7-13years). CT images were reconstructed with filtered back-projection (FBP), 50% adaptive statistical iterative reconstruction-Veo (50%ASIR-V), 100%ASIR-V, deep learning image reconstruction (DLIR) with low (DLIR-L), medium (DLIR-M), and high (DLIR-H) strengths. Subjective image quality was evaluated using a 5-point scale. CT value, noise, and sharpness of the trachea were measured. The VCAR software was used to automatically segment airways and reported the total volume. Segmentation success rates were recorded, and segmentation images were subjectively evaluated using a 6-point scale. ***Results:*** The average tracheal diameters were 8.53±1.88mm, 10.69±1.65mm, and 12.72±1.97mm, respectively for groups A, B, and C. The segmentation success rate depended on patient groups: group C reached 100%, while group A decreased significantly. In group A, 100%ASIR-V had the lowest rate at 7.69%, while DLIR-M and DLIR-H significantly improved the rate to 38.64% (P=0.03). For the segmented images, DLIR-H provided the lowest noise and highest subjective score while FBP images had the highest noise and 100%ASIR-V had the lowest overall score (P<0.05). There was no significant difference in the total airway volume among the six reconstructions. ***Conclusion:*** The airway segmentation success rate in ULD-CT for children depends on the tracheal size. DLIR improves airway segmentation success rate and image quality.

INTRODUCTION

CT is a commonly used imaging tool in clinical examination. Benefiting from the natural contrast between soft tissue and air, chest CT is the preferred way to evaluate airways and lung lesions [1-3]. With the continuous development of artificial intelligence (AI), automatic image segmentation has been used more for medical purposes. The technology of using big data to automatically segment and evaluate the lungs and airways continues to evolve [4-6], and its accuracy continues to rise [7, 8]. Improving the diagnosis speed [9] and reducing subjective error among doctors [10, 11] has become the direction of imaging development [12, 13]. Most of the existing clinical studies on AI, radiomics, and automatic segmentation of CT images have used standard radiation dose, and it is not clear how reduced radiation dose affects automatic segmentation results [4-13]. However, this is an important issue to address, since in CT examination, one should follow the principle of "as low as reasonably achievable" (ALARA principle) [14] to minimize radiation damage to patients during the CT process. The reduction of radiation dose will affect image quality. Furthermore, even if the same radiation dose is used, different reconstruction and post-processing algorithms will affect the image noise and image texture [15]. Will these changes in image quality affect the success rate and quality of the automatic segmentation, especially in the low radiation dose scan conditions? We wanted to add useful information by using ultra-low radiation dose chest CT images of children generated with different reconstruction algorithms, to identify factors that affect the success rate and effectiveness of automatic segmentation in clinical applications. Specifically, we wanted to investigate the impact of the newly developed deep learning image reconstruction (DLIR) algorithm.

[DOI: 10.61186/ijrr.22.1.171]

MATERIALS AND METHODS

General patient information

This study was a retrospective study and was approved by the ethics committee of Beijing Children's Hospital (registration number: 2019-46, date of registration: Aug 27, 2019), the informed consent was waived. In this study, 52 cases of chest CT with ultra-low dose CT (ULD-CT) protocol were continuously collected from February 1st, 2020 to August 31st, 2020 (table 1). There were 36 males and 16 females (average age 6.57±3.13 years, range 1-13 years). Patient inclusion criteria were: 1.

Follow-up chest CT (within 3 months of the routine enhanced chest CT) necessary for patients diagnosed as having thoracic malignant tumors; 2. Less than 18 years of age; 3. Patients had the stable conditions without new respiratory symptoms and rapid weight loss after the last chest CT examination.

Table 1. Patients' characteristics.

Characteristics	Average number, (range)
Male: female, n	36: 16
Ages, years	6.57 ± 3.13, (1.1-13.0)
70 kV group (1-2 years), n	13
80 kV group (3-6 years), n	19
100 kV group (7-13 years), n	20

CT data acquisition

All examinations were performed on a 256-row CT scanner (Revolution CT, GE HealthCare, USA). A patient age-dependent tube voltage protocol was used to maintain similar image noise across patient populations and minimize dose for younger patients: 70kV for patients of 1-2 years old; 80kV for patients of 3-6 years old; and 100kV for patients of 7-13 years old. A fixed tube current of 10mA (the lowest possible tube current selection on the scanner) was used. The gantry rotating speed was 0.35s/rot, the helical pitch value was 1.375:1, and the detector width was 40mm. Children were kept in a quiet state during CT scans. For those who could not cooperate, 10% chloral hydrate was given orally at a dose of 0.4ml/kg (by body weight), and the scan was not started until the child fell asleep.

CT data reconstruction

The ULD-CT raw data were reconstructed into six groups with different reconstruction algorithms: filtered back-projection (FBP), 50% adaptive statistical iterative reconstruction-Veo (ASIR-V), 100%ASIR-V, and deep learning image reconstruction (DLIR) with low (DLIR-L), medium (DLIR-M) and high (DLIR-H) strengths. A standard reconstruction kernel was used for all reconstructions, image thickness and spacing were 0.625mm, and no post-image reconstruction enhancement was applied.

Routine image quality evaluation

All images were transferred to an advantage workstation (AW4.7, GE HealthCare, USA). Two radiologists with 15 and 8 years of experience in pediatric diagnostic imaging were asked to perform the evaluation. The evaluation process was divided into the subjective evaluation and objective evaluation. The subjective evaluation also included the original CT images and the segmented bronchial tree.

The subjective evaluation for the original CT images used a 5-point scoring system. During the evaluation process, all patient information and scan parameters were shielded. The radiologists could freely adjust the window width and window level of the images according to personal habits, multiplanar reconstruction technique was also used to evaluate the airways. The two radiologists gave their scores independently. The subjective score was based on image noise, the display ability of the trachea and the bilateral bronchi, the clarity of airway walls. The scores of 3 points and higher were regarded as acceptable, and 5 points were the best.

The specific evaluation criteria were as follows: 5 points: low or no image noise, airways (trachea and bronchi and subsequent branches) had very clear boundaries, and tracheal diameter could be confidently and accurately measured, very strong diagnostic confidence; 4 points: low image noise, airways had clear boundaries and tracheal diameter could be accurately measured, strong diagnostic confidence; 3 points: moderate image noise, airways had slightly blurred boundaries, tracheal diameter could be measured, moderate diagnostic confidence; 2 points, high image noise, airways had blurred boundaries, tracheal diameter could not be confidently measured, low diagnostic confidence; 1 points: very high image noise, airways could not be confidently defined and tracheal boundaries could not be defined for measurement.

After the subjective evaluation, the two radiologists performed the conventional objective measurement together on the workstation: first, the slice at the aortic arch level was selected to measure the transverse diameter of the trachea; second, on the same image slice, a circular region of interest (ROI) with ¼ of the area of the trachea was placed in the center of the trachea (T) to measure its CT value and standard deviation (SD). The standard deviation was used to represent image noise. ROI of the same size was also used to measure the CT value and SD of mediastinal soft tissue (S). The signal-to-noise ratio (SNR) of the trachea was calculated as equations 1 and 2:

$$SNR = CT\ (T) / SD\ (T) \quad (1)$$

And contrast-to-noise ratio (CNR) was calculated

[DOI: 10.61186/ijrr.22.1.171]

as:

$$CNR = (CT(T) - CT(S)) / ((SD(T) + SD(S))/2) \quad (2)$$

Where; CT(T) and SD(T) represent the CT value and standard deviation of trachea, respectively, and CT(S) and SD(S) the CT value and standard deviation of mediastinal soft tissue, respectively.

The DICOM images of the same image slice were then transferred to a standalone computer to undergo the offline blur metric (BM) analysis [16]. The blur metric analysis quantifies the sharpness of image texture by comparing intensity variations between adjacent pixels of the original and low-pass-filtered images. The BM values are expressed as numeric values ranging from 0 to 1 with lower BM values indicating sharper images and more defined tracheal boundaries.

Segmentation and evaluation of bronchial tree

After finishing the routine measurement, the bronchial tree was automatically segmented by using the thoracic Volume Computer Assisted Reading (VCAR) software provided by AW4.7. The VCAR software automatically and intelligently identifies the bronchial tree; the software only retains and displays the bronchi and their subsequent branches, then deletes other pixels, and calculates the volume of all retained pixels. If the image quality is poor, VCAR will not make automatic segmentation and will display data errors. The success rate and image quality of the segmented bronchial tree images were evaluated and compared among different patient groups and reconstruction groups. The total volume of an entire bronchial tree was also noted and compared.

The automatic segmentation success rate refers to the ratio of the number of cases of successful bronchial tree segmentation without an error message after VCAR processing to the total number of cases in each of the patient group and reconstruction group. The subjective image quality evaluation of the segmented bronchial tree images was focused on the number of bronchi detected: 0 for the failed cases in the automatic segmentation; 1 for the main trachea and bilateral main bronchi only; 2 for 1-4 lobar main bronchi; 3 for a total 5 lobar bronchi; 4 for 1-5 segmental bronchi; 5 for 6-10 segmental bronchi and 6 for more than 10 sub-segmental bronchi.

Statistical analysis

All data were recorded, and continuous data were expressed as mean ± standard deviation. The Kolmogorov-Smirnov test was used to check for normal distribution, and analysis of variance with Bonferroni correction was used to compare whether there were statistical differences between different reconstruction algorithms. The Friedman test with Bonferroni correction was used to compare non-normally distributed continuous data and ordinal data such as image quality scores. The kappa test was used to evaluate the consistency of the subjective scores of the two radiologists. A $p<0.05$ was used to indicate a statistically significant difference.

RESULTS

There were 13 children in the 1-2 years age group (Group A), 19 children in the 3-6 years age group (Group B) and 20 children in the 7-13 years age group (Group C). The average volume CT dose index (CTDIvol) for the entire patient cohort was 0.07±0.03 mGy (0.04 – 0.10 mGy), 5% of the dose level based on the European Guidelines on Diagnostic Reference Levels for Paediatric Imaging [17], and the dose-length -product (DLP) was 1.81±0.84 mGy.cm. The average diameter of the trachea from the six reconstruction algorithms was 8.53±1.88 mm, 10.69±1.65 mm and 12.72±1.97 mm for children in groups A, B and C, respectively. There were significant differences in the average diameter of the trachea among different patient groups ($p<0.001$).

Evaluation of image quality of unsegmented images

Detailed results for the original CT images are shown in Table S2-6. The subjective image quality evaluation results for the original CT images showed that there were statistically significant differences among different reconstructions ($F=242.13$, $P<0.001$). DLIR-H had the best overall image quality with the tracheal wall being displayed and the lowest noise in the lumen, resulting in a median score of 4 points. 100%ASIR-V and FBP had the worst overall image quality scores, with no statistical difference between the two groups. Specifically, the 100% ASIR-V images had blurred tracheal walls, and FBP images had the highest image noise level.

The objective image quality results showed that there was no significant difference in the tracheal transverse diameter measurement results among different algorithms, and there was no significant difference in the CT values of the trachea and mediastinal soft tissue ($P =1.00$); However, there were significant differences in the SD measurement of the trachea and mediastinal soft tissue and SNR and CNR of trachea among different reconstructions (all $P<0.05$); DLIR-H and 100%ASIR-V had the best values in SD, SNR and CNR among groups but with no difference between them. The BM results showed that the lowest (best) value was with DLIR-L, followed by DLIR-M, 50%ASIR-V, DLIR-H, 100% ASIR-V and FBP. The results of DLIR-L in group A were the same as those of DLIR-M.

Evaluation results for the segmented bronchial tree

Detailed results for the segmented bronchial tree are shown in figure 1 and tables 2-4. There was no statistically significant difference in the overall

[DOI: 10.61186/ijrr.22.1.171]

success rate for the automatic image segmentation among the 6 reconstructions. However, the results in individual patient groups were different. The overall success rate was 25.64% (20/78), 67.54% (77/114) and 100% (120/120) for groups A, B and C, respectively. For Group A where the average diameter of the trachea was 8.53±1.88mm, 100% ASIR-V had the lowest success rate of 7.69% for the automatic image segmentation while DLIR-M and DLIR-H significantly improved the rate to 38.64% (P=0.03). For Group B, 100%ASIR-V also had the lowest value in the success rate among all reconstructions, but the differences were not statistically significant. Detailed success rates of automatic image segmentation with different reconstructions for different patient groups are listed in figure 1A.

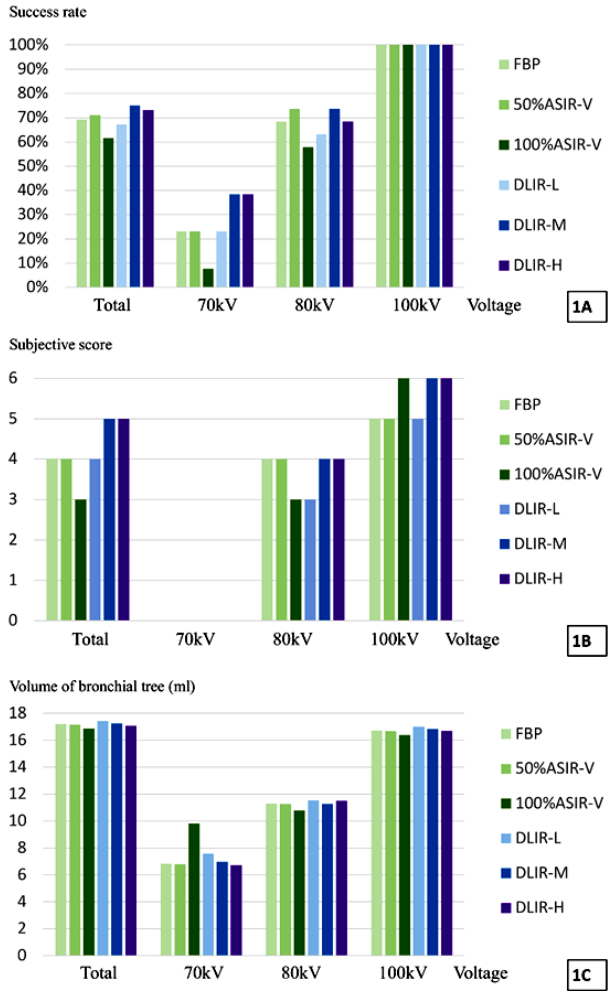

Figure 1. Detailed results for a segmented bronchial tree of six algorithm images: filtered back-projection (FBP), 50% adaptive statistical iterative reconstruction-Veo (ASIR-V), 100%ASIR-V, and deep learning image reconstruction (DLIR) with low (DLIR-L), medium (DLIR-M) and high (DLIR-H) strengths. **1A:** success rates of automatic image segmentation with different reconstructions for different sub-voltage groups; **1B:** subjective image quality scores of the automatically segmented bronchial tree with different reconstruction algorithms; and **1C:** total volumes of the bronchial tree with different algorithms.

The subjective evaluation of the segmented bronchial tree showed that DLIR-H and DLIR-M images were better than other reconstructions with more bronchial branches with a median score of 5 points. DLIR-L came second. 100%ASIR-V had the worst score (with a median score of 3 points) with distorted tracheal walls and incomplete bronchial branches. However, due to the low recognition rate of images in Group A, the median score for every reconstruction was 0 point for this group (the best average score was 1.77 with DLIR-H, and the worst score was 0.15 with 100%ASIR-V), even though DLIR images showed more bronchial branches (figure 1B). The airway volume obtained by automatic segmentation showed no statistical difference among different reconstructions ($P < 0.05$) (figure 1C).

The consistency of subjective scores of image quality was excellent with the Kappa value of 0.83, and the consistency of subjective scores for the segmented bronchial tree was excellent with the Kappa value of 0.92 between the two radiologists.

Table 2. Success rates of automatic image segmentation with different reconstructions for different sub-patient groups.

	FBP	50% ASIR-V	100% ASIR-V	DLIR-L	DLIR-M	DLIR-H
total	69.23% (36/52)	71.15% (37/52)	61.54% (32/52)	67.31% (35/52)	75% (39/52)	73.08% (38/52)
70kV	23.08% (3/13)	23.08% (3/13)	7.69% (1/13)	23.08% (3/13)	38.46% (5/13)	38.46% (5/13)
80kV	68.42% (13/19)	73.68% (14/19)	57.89% (11/19)	63.16% (12/19)	73.68% (14/19)	68.42% (13/19)
100kV	100.00% (20/20)	100.00% (20/20)	100.00% (20/20)	100.00% (20/20)	100.00% (20/20)	100.00% (20/20)

FBP: filtered back-projection; ASIR-V: Adaptive Statistical Iterative Reconstruction-V; DLIR: Deep learn image reconstruction; DLIR-L: DLIR with low strength; DLIR-M: DLIR with medium strength; DLIR-H: DLIR with high strength.

[DOI: 10.61186/ijrr.22.1.171]

Table 3. Subjective image quality scores of the automatically segmented bronchial tree with different reconstruction algorithms.

algorithm	score	total		70kV		80kV		100kV	
		median score	No. (percentage)	median score	No. (percentage)	median score	No. (percentage)	median score	No. (percentage)
FBP	0	4	32 (30.77%)	0	20 (76.92%)	4	12 (31.58%)	5	0 (0.00%)
	1		0 (0.00%)		0 (0.00%)		0 (0.00%)		0 (0.00%)
	2		3 (2.88%)		3 (11.54%)		0 (0.00%)		0 (0.00%)
	3		9 (8.65%)		3 (11.54%)		6 (15.79%)		0 (0.00%)
	4		18 (17.31%)		0 (0.00%)		18 (47.37%)		0 (0.00%)
	5		37 (35.58%)		0 (0.00%)		2 (5.26%)		35 (87.5%)
	6		5 (4.81%)		0 (0.00%)		0 (0.00%)		5 (12.5%)
50%ASIR-V	0	4	30 (28.85%)	0	20 (76.92%)	4	10 (26.32%)	5	0 (0.00%)
	1		0 (0.00%)		0 (0.00%)		0 (0%)		0 (0.00%)
	2		4 (3.85%)		4 (15.38%)		0 (0%)		0 (0.00%)
	3		6 (5.77%)		2 (7.69%)		4 (10.53%)		0 (0.00%)
	4		20 (19.23%)		0 (0.00%)		20 (52.63%)		0 (0.00%)
	5		40 (38.46%)		0 (0.00%)		4 (10.53%)		36 (90.0%)
	6		0 (0.00%)		0 (0.00%)		0 (0.00%)		4 (10.0%)
100%ASIR-V	0	3	40 (38.46%)	0	24 (92.31%)	3	16 (42.11%)	6	0 (0.00%)
	1		0 (0.00%)		0 (0.00%)		0 (0.00%)		0 (0.00%)
	2		2 (1.92%)		2 (7.69%)		0 (0.00%)		0 (0.00%)
	3		10 (9.62%)		0 (0.00%)		10 (26.32%)		0 (0.00%)
	4		10 (9.62%)		0 (0.00%)		10 (26.32%)		0 (0.00%)
	5		20 (19.23%)		0 (0.00%)		2 (5.26%)		18 (45.0%)
	6		22 (21.15%)		0 (0.00%)		0 (0.00%)		22 (55.0%)
DLIR-L	0	4	34 (32.69%)	0	20 (76.92%)	3	14 (36.84%)	5	0 (0.00%)
	1		0 (0.00%)		0 (0.00%)		0 (0.00%)		0 (0.00%)
	2		0 (0.00%)		0 (0.00%)		0 (0.00%)		0 (0.00%)
	3		10 (9.62%)		0 (0.00%)		10 (26.32%)		0 (0.00%)
	4		16 (15.38%)		4 (15.38%)		12 (31.58%)		0 (0.00%)
	5		36 (34.62%)		2 (7.69%)		2 (5.26%)		32 (80.0%)
	6		8 (7.69%)		0 (0.00%)		0 (0.00%)		8 (20.0%)
DLIR-M	0	5	26 (25%)	0	16 (61.54%)	4	10 (26.32%)	6	0 (0.00%)
	1		0 (0.00%)		0 (0.00%)		0 (0.00%)		0 (0.00%)
	2		0 (0.00%)		0 (0.00%)		0 (0.00%)		0 (0.00%)
	3		2 (1.92%)		0 (0.00%)		2 (5.26%)		0 (0.00%)
	4		22 (21.15%)		4 (15.38%)		18 (47.37%)		0 (0.00%)
	5		16 (15.38%)		6 (23.08%)		6 (15.79%)		4 (10.0%)
	6		38 (36.54%)		0 (0.00%)		2 (5.26%)		36 (90.0%)
DLIR-H	0	5	28 (26.92%)	0	16 (61.54%)	4	12 (31.58%)	6	0 (0.00%)
	1		0 (0.00%)		0 (0.00%)		0 (0.00%)		0 (0.00%)
	2		0 (0.00%)		0 (0.00%)		0 (0.00%)		0 (0.00%)
	3		2 (1.92%)		0 (0.00%)		2 (5.26%)		0 (0.00%)
	4		21 (20.19%)		5 (19.23%)		16 (42.11%)		0 (0.00%)
	5		15 (14.42%)		5 (19.23%)		6 (15.79%)		4 (10.0%)
	6		38 (36.54%)		0 (0.00%)		2 (5.26%)		36 (90.0%)

FBP: filtered back-projection; ASIR-V: Adaptive Statistical Iterative Reconstruction-V; DLIR: Deep learn image reconstruction; DLIR-L: DLIR with low strength; DLIR-M: DLIR with medium strength; DLIR-H: DLIR with high strength.

Table 4. The total volume of bronchial tree automatically segmented by VCAR software with different algorithms.

VCAR volume (ml)	FBP	50%ASIR-V	100%ASIR-V	DLIR-L	DLIR-M	DLIR-H
total	17.22±6.94	17.16±6.96	16.87±6.75	17.43±6.67	17.24±6.61	17.07±6.64
70kV	6.85±3.62	6.81±3.52	9.81±0.00	7.50±4.17	6.96±3.09	6.72±3.06
80kV	11.29±3.53	11.26±3.34	10.78±3.34	11.54±3.62	11.28±3.54	11.49±3.35
100kV	16.71±6.94	16.67±6.96	16.38±6.75	17±6.67	16.82±6.61	16.69±6.64

DISCUSSION

In this study, we investigated the impact of tracheal size and different reconstruction algorithms on the success rate and quality of automatic segmentation of bronchial tree of pediatric patients in ultra-low radiation dose conditions. Automatic image segmentation is widely used [16], especially for organizations with large contrast and good boundary [18-20], such as CT angiography, and CT Colonography. With the application of radiomics and AI technology, the accuracy of automatic segmentation algorithms has been improved [21-22], but image quality remains an important factor limiting the success rate of automatic segmentation [23]. However, most studies have not described the influence of radiation dose and image reconstruction algorithms on automatic segmentation, especially for pediatric patients with

[DOI: 10.61186/ijrr.22.1.171]

smaller trachea and bronchi. Although there have been recent reports that the use of the DLIR algorithm can improve the automatic detection rate of pulmonary nodules [24], there is no analysis of how DLIR improves the automatic segmentation effect, and there is a lack of in-depth research on the impact of CT image quality on automatic segmentation. Following the ALARA principle in radiation dose, we tried to maintain similar image noise (when using the same reconstruction algorithm) for different patients in our study to minimize the influence of image noise on the automatic segmentation success rate.

Our results implied that image noise alone might not be the major factor impacting the success rate of segmenting bronchial trees, since all three patient groups had similar image noise, but drastically different success rate in automatic segmentation, when the same reconstruction was applied, so we believe the success rate was mainly driven by the different tracheal diameters.

Further analysis of the results also indicated that for patients with small size trachea (< 10mm in diameter) and bronchia, the combination of image noise and sharpness generated by different reconstruction algorithms might have a significant impact on the segmentation success rate and image quality of segmented bronchial trees. For the patient group with the smallest tracheal size, 100%ASIR-V images, which had the second lowest image noise among the six reconstruction groups, had the lowest success rate at 7.69%, while DLIR-M and DLIR-H significantly improved the success rate to 38.46%.

Previous studies have shown that a higher percentage of ASIR-V significantly changes the noise-power-spectrum (NPS) in images when reducing noise, reducing the peak frequency which causes blurred image edges, coarser image noise presentation and “plastic”-looking image appearance that may affect diagnosis [25]. On the other hand, the DLIR algorithm uses deep learning to directly remove noise in generating images, and better maintains image texture and high-frequency information to provide clearer tissue boundaries than the ASIR-V algorithm [26].

In our study, we further verified our findings using the blur matrix and found that DLIR images had either only slightly higher (DLIR-M) or lower image noise (DLIR-H) compared with 100%ASIR-V images, but much lower blur matrix values. With a better balance of image noise and sharpness (figures 2 and 3), the success rates of automatic segmentation were higher. Taking into account previous research results [23] showing the use of DLIR algorithm can improve the success rate of automatic segmentation of lung nodules and small airways, our results further supported the hypothesis that by improving image texture, reconstruction algorithms, such as DLIR, could further improve the success rate of automatic segmentation.

There are still some limitations in this study. Firstly, the sample size in the 70kv group was small, and the problem of low automatic segmentation success rate was not fully considered, resulting in too few cases in the 70kv group; Secondly, the low dose protocols were set according to age, so it was impossible to compare the differences among different dose levels on the same group of children, therefore the dependence on radiation dose; Finally, we only applied one automatic segmentation software and the robustness with other automatic segmentation software needs further study.

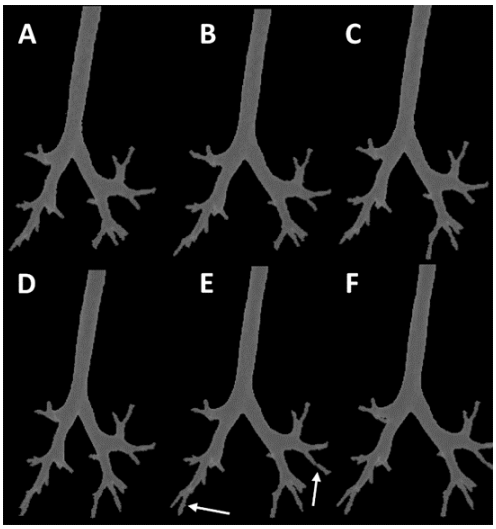

Figure 2. Automatic segmentation with VCAR software of a 9-years old boy of six algorithm images: filtered back-projection (FBP, figure 2A), 50% adaptive statistical iterative reconstruction-Veo (ASIR-V, figure 2B), 100%ASIR-V (figure 2C), and deep learning image reconstruction (DLIR) with low (DLIR-L, figure 2D), medium (DLIR-M, figure 2E) and high (DLIR-H, figure 2F) strengths. Scan voltage was 100kV with 0.10mGy in CT dose index. Compared with other images, DLIR-H and DLIR-M images showed more bronchi (arrows).

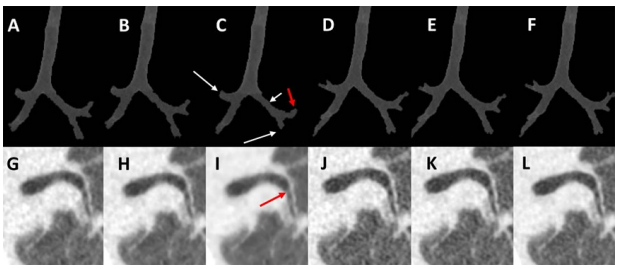

Figure 3. 3A-3E are automatic segmentation images of VCAR software and 3G-3L are multi-planar reformat images of a 2-years old boy. Scan voltage was 70kV with 0.04mGy in the CT dose index. 3A and 3G: filtered back-projection images, 3B and 3H: 50% adaptive statistical iterative reconstruction-Veo (ASIR-V) images, 3C and 3I: 100%ASIR-V images, 3D and 3J: deep learning image reconstruction (DLIR) with low strength images, 3E and 3K: with medium strength, 3F and 3L: with high strength. Compared with other images, the left main bronchus of 100%ASIR-V was distorted and smaller (short arrow), there were fewer bronchial branches (long arrow), and the image quality was too smooth and blotchy. DLIR image could show more bronchi.

[DOI: 10.61186/ijrr.22.1.171]

CONCLUSION

The airway segmentation success rate in ULD-CT for children depends on the tracheal size. DLIR improves the success rate and image quality of airway segmentation which are affected by both image noise and sharpness.

ACKNOWLEDGMENTS

The authors would like to thank Dr. Jianying Li and Dr. Luotong Wang for their help to generate DLIR images and for further understanding of the automatic airway segmentation technique, and thank Dr. Zhuoheng Liu for his help to calculate blur matrix values and analyzing the results.

***Competing interests*:** The authors declare no competing interests.

***Conflict of interest*:** The authors declare that they have no conflict of interest.

***Ethics approval and consent to participate*:** This retrospective study was approved by the Ethics Committees of Beijing Children's Hospital for using the data, and the informed consent was waived.

***Consent for publication*:** Not applicable.

***Authors' contributions*:** J Sun: Project development, Data Collection, Manuscript writing; H Li: Data Collection, Manuscript writing; Z Liu: Data Collection, Manuscript writing; S Wang: Data analysis, Manuscript editing; M Li: Data analysis, Manuscript editing; Y Peng: Manuscript editing

***Funding*:** Beijing Municipal Administration of Hospitals Incubating Program (PX2022050).

***Data availability*:** Not applicable.

REFERENCES

1. Sun J, Chen C, Peng Y, *et al.* (2019) Comparison of magnetic resonance imaging and computed tomography to measure preoperative parameters of children with pectus excavatum. *Pediatric Investigation, **3**(2): 102-109*.
2. He M, Wang C, Xu L, *et al.* (2020) Epidemiological and clinical characteristics of 35 children with COVID-19 in Beijing, China. *Pediatric Investigation, **4**(4): 230-235*.
3. Ye Z, Zhang Y, Wang Y, *et al.* (2020) Chest CT manifestations of new coronavirus disease 2019 (COVID-19): a pictorial review. *European radiology, **30**(8): 4381-4389*.
4. Yun J, Cho YH, Lee SM, *et al.* (2021) Deep radiomics-based survival prediction in patients with chronic obstructive pulmonary disease. *Scientific Reports, **11**(1): 15144*.
5. Tanabe N, Sato S, Oguma T, *et al.* (2019) Associations of airway tree to lung volume ratio on computed tomography with lung function and symptoms in chronic obstructive pulmonary disease. *Respiratory Research, **20**(1): 77*.
6. Kan CNE, Gilat-Schmidt T, Ye DH (2021) Enhancing reproductive organ segmentation in pediatric CT via adversarial learning. *Proceedings of SPIE--the International Society for Optical Engineering, **11596**: 1159612*.
7. Shujaat S, Jazil O, Willems H, *et al.* (2021) Automatic segmentation of the pharyngeal airway space with convolutional neural network. *Journal of Dentistry, **111**: 103705*.
8. Handa T, Tanizawa K, Oguma T, *et al.* (2022) Novel artificial intelligence-based technology for chest computed tomography analysis of idiopathic pulmonary fibrosis. *Annals of the American Thoracic Society, **19**(3): 399-406*.
9. Garrett Fernandes M, Bussink J, Stam B, *et al.* (2021) Deep learning model for automatic contouring of cardiovascular substructures on radiotherapy planning CT images: Dosimetric validation and reader study based clinical acceptability testing. Radiotherapy and oncology: *Journal of the European Society for Therapeutic Radiology and Oncology, **165**: 52-59*.
10. Fischer AM, Varga-Szemes A, van Assen M, *et al.* (2020) Comparison of artificial intelligence-based fully automatic chest ct emphysema quantification to pulmonary function testing. *AJR. American Journal of Roentgenology, **214**(5): 1065-1071*.
11. Nambu A, Zach J, Schroeder J, *et al.* (2016) Quantitative computed tomography measurements to evaluate airway disease in chronic obstructive pulmonary disease: Relationship to physiological measurements, clinical index and visual assessment of airway disease. *European Journal of Radiology, **85**(11): 2144-2151*.
12. Kirby M, Tanabe N, Tan WC, *et al.* (2018) CanCOLD collaborative research group, Canadian respiratory research network, & CanCOLD collaborative research group, the Canadian respiratory research network (2018). Total airway count on computed tomography and the risk of chronic obstructive pulmonary disease progression. Findings from a population-based study. *American Journal of Respiratory and Critical Care Medicine, **197**(1): 56-65*.
13. Mao L, Chen H, Liang M, *et al.* (2019) Quantitative radiomic model for predicting malignancy of small solid pulmonary nodules detected by low-dose CT screening. *Quantitative Imaging in Medicine and Surgery, **9**(2): 263-272*.
14. Sun J, Li H, Li J, *et al.* (2021) Performance evaluation of using shorter contrast injection and 70 kVp with deep learning image reconstruction for reduced contrast medium dose and radiation dose in coronary CT angiography for children: a pilot study. *Quantitative Imaging in Medicine and Surgery, **11**(9), 4162-4171*.
15. Sun J, Li H, Li J, *et al.* (2021) Improving the image quality of pediatric chest CT angiography with low radiation dose and contrast volume using deep learning image reconstruction. *Quantitative Imaging in Medicine and Surgery, **11**(7): 3051-3058*.
16. Park C, Choo KS, Jung Y, *et al.* (2021) CT iterative vs deep learning reconstruction: comparison of noise and sharpness. *European Radiology, **31**(5): 3156-3164*.
17. Almén A, Guðjónsdóttir J, Heimland N,et al. (2022). Paediatric diagnostic reference levels for common radiological examinations using the European guidelines. *The British journal of radiology, 95 **(1130):** 20210700.*
18. Wei X, Chen X, Lai C, *et al.* (2021) Automatic liver segmentation in CT images with enhanced GAN and mask region-based CNN architectures. *BioMed Research International, 2021, 9956983*.
19. Zeng G, Degonda C, Boschung A, *et al.* (2021) Three-dimensional magnetic resonance imaging bone models of the hip joint using deep learning: Dynamic simulation of hip impingement for diagnosis of intra- and extra-articular hip impingement. *Orthopaedic Journal of Sports Medicine, **9**(12): 23259671211046916*.
20. Song J, Huang SC, Kelly B, *et al.* (2022) Automatic lung nodule segmentation and intra-nodular heterogeneity image generation. *IEEE Journal of Biomedical and Health Informatics, **26**(6): 2570-2581*.
21. Ko H, Huh J, Kim KW, *et al.* (2022). A deep residual U-net algorithm for automatic detection and quantification of ascites on abdominopelvic computed tomography images acquired in the emergency department: Model development and validation. *Journal of Medical Internet Research, **24**(1): e34415*.
22. Beekman C, van Beek S, Stam J, *et al.* (2022) Improving predictive CTV segmentation on CT and CBCT for cervical cancer by diffeomorphic registration of a prior. *Medical Physics, **49**(3): 1701-1711*.
23. Huang Y, Hu G, Ji C, Xiong H (2020) Glass-cutting medical images via a mechanical image segmentation method based on crack propagation. *Nat Commun, **11**(1): 5669.*
24. Jiang B, Li N, Shi X, *et al.* (2022) Deep learning reconstruction shows better lung nodule detection for ultra-low-dose chest CT. *Radiology, **303**(1): 202-212*.
25. Sui X, Meinel FG, Song W, *et al.* (2016) Detection and size measurements of pulmonary nodules in ultra-low-dose CT with iterative reconstruction compared to low dose CT. *European Journal of Radiology, **85**(3): 564-570*.
26. Greffier J, Hamard A, Pereira F, *et al.* (2020) Image quality and dose reduction opportunity of deep learning image reconstruction algorithm for CT: a phantom study. *European Radiology, **30**(7): 3951-3959*.

[DOI: 10.61186/ijrr.22.1.171]